NACACASE FIL COPY

RESEARCH MEMORANDUM

FORCE TEST RESULTS FOR BODY-MOUNTED

LATERAL CONTROLS AND SPEED BRAKES ON A 45° SWEPT-W

MODEL AT MACH NUMBERS FROM 0.80 TO 0.98

By F. E. West, Jr., and Chris C. Critzos

Langley Aeronautical Laboratory Langley Field, Va.

CLASSIFIED DOCUMENT

This material contains information affecting the National Defense of the United States within the meaning of the espionage laws, Title 18, U.S.C., Secs. 793 and 794, the transmission or revelation of which in any manner to an unauthorized person is prohibited by law.

NATIONAL ADVISORY COMMITTEE FOR AERONAUTICS

WASHINGTON

December 5, 1956

CONFIDENTIAL

NATIONAL ADVISORY COMMITTEE FOR AERONAUTICS

RESEARCH MEMORANDUM

FORCE TEST RESULTS FOR BODY-MOUNTED

LATERAL CONTROLS AND SPEED BRAKES ON A 45° SWEPT-WING

MODEL AT MACH NUMBERS FROM 0.80 TO 0.98

By F. E. West, Jr., and Chris C. Critzos

SUMMARY

An investigation has been made in the Langley 16-foot transonic tunnel to determine the aerodynamic characteristics of several body-mounted lateral-control and speed-brake configurations. The basic model had a 45° swept wing with an aspect ratio of 3. Six-component balance data were obtained at Mach numbers of 0.80, 0.94, and 0.98 for angles of attack that usually ranged from about 0° to 21°.

At large deflections, oppositely deflected body-mounted lateral controls produce fairly large rolling moments at low and moderate angles of attack even when the speed brakes are deflected 0.2 of the wing semispan. Shifting the hinge lines of the controls from 100 to 85 percent of the wing chord at the fuselage results in higher roll effectiveness at low control deflections. Adding a complete tail to the model with oppositely deflected controls at large deflections results in a change from unfavorable to favorable yawing moments and in a decrease in roll effectiveness.

INTRODUCTION

With the trend toward very thin wings of low aspect ratio, the support of lateral controls on wings is becoming a difficult problem. This problem involves both space and control load considerations. For configurations with such small wings, it may be desirable to use fuselage-mounted lateral controls. Hence, preliminary test results have been obtained in the Langley 16-foot transonic tunnel on one possible type of fuselage-mounted lateral control. This type of control, referred to as a body-mounted lateral control, is similar to a fuselage-mounted speed brake. Upper and lower controls are located on each side of an aircraft fuselage in the vicinity of the wing trailing

CONFIDENTIAL

edge so as to influence the wing flow field. In order to obtain roll, the upper control on one side of the fuselage and the lower control on the opposite side of the fuselage are deflected. For speed-brake purposes, all four controls can be deflected simultaneously.

These controls were tested on a sting-supported 45° swept-wing model having a 4-percent-thick wing of aspect ratio 3. Six-component balance data and wing static pressures were obtained at Mach numbers of 0.80, 0.94, and 0.98 for angles of attack up to 21°. The results obtained from the balance are presented in this paper. Aerodynamic characteristics are shown for configurations with oppositely deflected body-mounted lateral controls at various deflections. Also shown are the effects on the aerodynamic characteristics of reducing control span, shifting control hinge-line locations, deflecting speed brakes, and of adding a complete tail to the model.

SYMBOLS

Forces are referenced to the wind axes and the moments are presented about the body axes. These systems have their origin at a point in the plane of symmetry which corresponds to the 25-percent-chord station of the mean aerodynamic chord.

ъ	wing span
c	local wing chord
e_{b}	wing chord at wing-fuselage intersection
ē	mean aerodynamic chord
$^{\rm C}{}_{ m D}$	drag coefficient, $\frac{\text{Drag}}{\text{qS}}$
$\mathtt{c}_{\mathtt{L}}$	lift coefficient, $\frac{\text{Lift}}{\text{qS}}$
Cl	rolling-moment coefficient produced by controls, Rolling moment qSb
$C_{\mathbf{m}}$	pitching-moment coefficient, Pitching moment

CONFIDENTIAL

qSc

δ

C _n	yawing-moment coefficient, produced by controls, Yawing moment 4Sb
$^{\mathrm{C}}\mathbf{Y}$	lateral-force coefficient produced by controls, <u>Lateral force</u> qS
$^{\mathrm{c}_{\mathrm{p}_{\mathrm{b}}}}$	base pressure coefficient, $\frac{p_b - p}{q}$
D_{max}	maximum body diameter
М	free-stream Mach number
р	static pressure at base of model
p	free-stream static pressure
q	free-stream dynamic pressure
S	total wing area
у	lateral distance extending outboard from control hinge lines
α	angle of attack of fuselage center line

 $\Delta C_{\mathrm{D}}, \ \Delta C_{\mathrm{L}}, \ \Delta C_{\mathrm{m}}$ incremental coefficients produced by controls

control deflection

APPARATUS

Tunnel and Model

The investigation was made in the Langley 16-foot transonic tunnel. A description of this facility and its air-flow and power characteristics are presented in reference 1.

Dimensional details of the model are given in figure 1. The basic model has been tested previously (see refs. 2 and 3). The aluminumalloy wing, steel horizontal tail, and plastic vertical tail had their quarter-chord lines swept 45°. The wing had an aspect ratio of 3, a taper ratio of 0.2, and NACA 65AOO4 airfoil sections. It was mounted in a midwing position on the fuselage and had no incidence, dihedral,

CONFIDENTIAL .

or twist. The steel fuselage consisted of a body of revolution with a fineness ratio of 10.95. (See ref. 3 for fuselage ordinates.) The model was mounted on the sting-support system described in reference 4.

Body-Mounted Lateral Controls and Speed Brakes

Figure 2 shows two views of a lower right body-mounted lateral control at full deflection with the hinge line at the intersection of the wing trailing edge and the body. For most configurations, the controls were pivoted about vertical hinge lines located at this point. This arrangement is also indicated in the model plan-form sketch of figure 1 by the dashed lines showing a body lateral control at several deflections. As shown in figure 1, deflection was measured in terms of the wing semispan. Each control, when at full deflection (that is, rotated forward to the wing trailing edge) usually had a projected span of 0.3 b/2 and a projected height of 0.1c. For one configuration, however, the projected span at full deflection was reduced to 0.2 b/2. Each of these controls had one edge on the wing chord plane extended for all control deflections.

For another lateral-control configuration, the control hinge lines were moved forward to the intersection of the wing 85-percent-chord line with the body. At full deflection, each of these controls had their length parallel to the wing trailing edge and one edge that corresponded to the local wing surface. Since these controls rotate about vertical hinge lines, gaps existed between the controls and the wing surface at the lower deflections.

Although the controls consisted of flat steel plate, their chord lines were swept back (see fig. 2(b)) to approximate the slope the controls would have if contoured to correspond to the body surface in the retracted position. That is, the control chord lines were swept back 12.4° from vertical lines in planes that were perpendicular to the control front faces.

TESTS

The various lateral-control and speed-brake configurations used in the present tests are indicated in table I. (The control deflections of 0.1 b/2, 0.2 b/2, and 0.3 b/2 shown in table I correspond to deflection angles, with respect to the plane of symmetry, of 18.55° , 39.24° , and 71.56° , respectively.) Each configuration was tested at Mach numbers of 0.80, 0.94, and 0.98. Angle of attack was usually varied from about 0° to 21° . However, because of balance limitations, the maximum angle of attack was about 17° at a Mach number of 0.98 for the tail-on configurations.

The variation of Reynolds number with Mach number is presented in figure 3.

PRECISION

The lift and drag data have been adjusted to a condition of free-stream static pressure at the fuselage base. Base pressures were obtained by averaging measurements from three static-pressure orifices spaced equidistantly around the base annulus just inside the fuselage base. Configuration changes resulted in a large range of base pressure coefficients at each test condition. The variation of this range with angle of attack is shown in figure 4 for each Mach number. Generally the configurations with speed brakes or lateral controls at full deflection had the lowest base pressure coefficients, whereas the configurations with undeflected controls had the highest base pressure coefficients. (A base pressure coefficient of 0.1 is equivalent to a drag coefficient of 0.0026.)

Except for the base-pressure adjustments, sting interference effects have been neglected. The neglected sting interference effects which may affect the flow over the fuselage afterbody and over the tail are believed to be small.

Tunnel-wall effects are small for the Mach number range of the present investigation (see ref. 5) and have also been neglected.

The accuracy of the aerodynamic coefficients based on balance precision and repeatability of data is believed to be within the following limits:

C_	
$^{ m C_L}$	±0.01
C_D at low angles of attack	
	± 0.001
CD at high angles of attack	±0.005
c_{m}	+0.005
C	_0.00)
$c_1 \dots \dots \dots$	±0.001
c_n	+0 001
	±0.001
c_{Y}	±0.00 2

Angle-of-attack accuracy is estimated to be within ±0.1°.

RESULTS AND DISCUSSION

The longitudinal aerodynamic characteristics for the basic tailoff and tail-on models are presented in figure 5. (The solid symbols
indicated in the various figures are reference points used in machine
plotting.) The primary purpose of figure 5 is to show the basic-model
longitudinal data used as a basis for obtaining incremental changes
due to deflection of the various lateral controls and speed brakes.
Longitudinal aerodynamic characteristics for the basic model with and
without the horizontal tail have been discussed in reference 2.

The figures showing the aerodynamic characteristics due to deflection of the various body-mounted lateral controls (figs. 6 to 11) or speed brakes (fig. 12) are indicated in table I. Curves shown in figure 6 for the oppositely deflected lateral controls at $\delta = 0.3$ b/2 are repeated in figures 7 to 11 for comparative purposes. Summary curves showing the variation of rolling-moment coefficient with control deflection for several of the body-mounted lateral-control configurations are presented in figure 13.

Lateral-Control Effectiveness With Tail Off

Oppositely deflected controls with hinge lines at $1.00c_b$. Figure 6(a) shows that at low and moderate angles of attack the oppositely deflected controls with hinge lines at $1.00c_b$ produced fairly large rolling moments when fully deflected ($\delta = 0.3 \text{ b/2}$). Reversals or large losses in control effectiveness occurred in the angle-of-attack range near 20° . In this angle range, flow separation on the wing upper surface would be expected to have an adverse effect on lateral-control effectiveness.

At the smaller control deflections ($\delta = 0.1$ b/2 and 0.2 b/2), control effectiveness was rather low. (See fig. $\delta(a)$.) One reason for this low effectiveness is that the controls were rather remote from the wing at the smaller deflections. For such body controls it would appear that the variation of rolling-moment coefficient with control deflection should be some function of the sine squared of the deflection angle. Not only does the lift change with control deflection, but also the center of lift shifts spanwise with control deflection. By contrast the rolling-moment coefficient of a conventional aileron is a function of the sine of the deflection angle.

At the smallest deflection ($\delta = 0.1 \text{ b/2}$), there were no indications of reversals in control effectiveness at the low angles of attack. Whether or not reversals may occur at deflections smaller than 0.1 b/2

is not known. Such reversals, however, if they did occur, would be very small. (See figs. 6(a) and 13.) It is presumed that the power actuators of such a control system would be programmed to move the controls very rapidly through the low deflection range and control reversals would, therefore, be of negligible importance.

Figure 6(a) also shows that Mach number effects on control effectiveness were usually small except for the fully deflected condition at high angles of attack.

Individually deflected controls with hinge lines at $1.00c_b$.Individual controls were tested to determine the relative contribution of the separate segments of the oppositely deflected controls. Figure 7(a) shows that the summation of the rolling-moment coefficients due to these individual controls closely approximate the values due to the oppositely deflected controls. Unfortunately, the lower control was not tested beyond 12^O angles of attack.

As shown in figure 7(a) the upper control segment was responsible for the loss in effectiveness of the oppositely deflected controls when the angle of attack was increased to moderate values. The upper control configuration also suffered control reversals at the higher angles of attack. The losses in upper control effectiveness are apparently the result of flow separation which starts in the vicinity of the wing tip and spreads over the wing upper surface as the angle of attack is increased. (See ref. 3.)

Study of the curves for the upper control and oppositely deflected control configurations can give an indication of the lower control effectiveness at the higher angles of attack. (See fig. 7(a).) From the trend of these curves and the differences between them it is apparent that the lower control would generally have a higher effectiveness than the upper control at the higher angles of attack. These curves also indicate, however, that a reversal in lower control effectiveness may occur at about 20° angle of attack for a Mach number of 0.94. At the other Mach numbers there are no indications of reversals in lower control effectiveness within the range of the data.

Oppositely deflected controls with hinge lines at $0.85c_b$.— Shifting the hinge lines of the oppositely deflected controls from $1.00c_b$ to $0.85c_b$ improved significantly the control effectiveness at the low control deflections. (See fig. 13.) This improvement apparently resulted from the control surfaces being moved into a higher velocity portion of the wing flow field at low deflections. Shifting the hinge lines, however, decreased control effectiveness at the larger control deflections. (See figs. 8(a) and 13.) This decrease was probably the result of flow separation on the large wing areas lying between the controls

and the wing trailing edge. Hence, while a body control produces rolling moment by causing pressure increases on the wing surface lying ahead of it, the flow separation causes pressure decreases on the wing surface lying behind the control. (Ref. 6 shows a similar effect of spoiler ailerons on wing pressures.)

Reduced control span with hinge lines at $1.00c_b$. The effects of reducing the spans of the oppositely deflected controls by 33 percent at full deflection were to reduce control effectiveness at low angles of attack about 20 percent. (See fig. 9(a).) At high angles of attack the effectiveness of the shorter span controls approached or exceeded the effectiveness of the longer span controls.

Oppositely deflected controls and speed brakes with hinge lines at 1.00c_b.- The primary purpose of figure 10 is to indicate the effectiveness of the body lateral controls with speed brakes deflected. For this discussion the control positions defined in table I for figure 10 will be referred to as the condition with the oppositely deflected lateral controls deflected to 0.3 b/2 from a speed brake position of 0.2 b/2.

At low angles of attack figure 10(a) shows that deflecting the speed brakes resulted in a maximum reduction in control effectiveness of about 20 percent. However, the body controls still produced fairly large rolling moments. Essentially, the speed brakes corresponded to one pair of lateral controls at a deflection of 0.2 b/2 whose roll effectiveness tended to oppose that of the pair of fully deflected lateral controls. Hence, as would be expected, the reductions in control effectiveness shown in figure 10(a) corresponded approximately to the rollingmoment coefficients shown in figure 6(a) for the oppositely deflected controls at a deflection 0.2 b/2.

Other Lateral-Control Effects With Tail Off

Yawing-moment characteristics. Figure 6(a) shows that the oppositely deflected controls produced unfavorable yawing-moment coefficients. As shown in figure 7(a), the lower control was primarily responsible for the unfavorable values. For the largest deflection $(\delta=0.3~b/2)$, shifting the control hinge lines from $1.00c_b$ to $0.85c_b$ generally had the effect of decreasing the absolute magnitude of the yawing-moment coefficient at Mach numbers of 0.94 and 0.98 (fig. 8(a)). A similar effect was obtained at all Mach numbers when the speed brakes were deflected 0.2~b/2. (See fig. 10(a).) However, as indicated in figure 9(a), the reduction in control span had only minor effects on the yawing-moment coefficients.

Side-force characteristics. - The side-force coefficients shown in figure 6(a) for the oppositely deflected controls were positive and generally increased with Mach number. Shifting the control hinge lines, deflecting the speed brakes, or reducing control span had effects on side force that were similar to those discussed for yawing moment.

Lift and pitching-moment characteristics.— The incremental lift and pitching-moment coefficients due to deflecting the oppositely deflected controls 0.3 b/2 were fairly large (particularly ΔC_m) at moderately high angles of attack. (See fig. 6(b).) As indicated in figure 7(b) these increments were due to the lower control contributing most of the effectiveness.

Of the various changes in control configuration, shifting the hinge lines of the oppositely deflected controls from $1.00c_b$ to $0.85c_b$ had the largest effect on the incremental coefficients for a control deflection of $0.3\ b/2$. This shifting of the hinge lines resulted in reversals in the signs of the incremental lift and pitching-moment coefficients at the moderate and high angles of attack. (See fig. 8(b).) The reversals indicate that the upper control had become more effective than the lower control at these angles of attack. Apparently, flow separation on the wing surfaces behind the controls had a more detrimental effect on lower control effectiveness than on upper control effectiveness.

Thus, the results in figure 8(b) indicate that a hinge-line location between $0.85c_b$ and $1.00c_b$ can probably be selected so that the lift and pitching moment due to control deflection will be small at all angles of attack; that is, the effectiveness of the control will be almost equally shared by the upper and lower controls at all angles of attack.

Drag characteristics. - As indicated in figures 6(b), 7(b), 8(b), 9(b), and 10(b), the incremental drag coefficients for the various controls were large. However, these large values are not considered to be of concern since lateral controls are deflected for only brief periods of time. (See ref. 7.)

Lateral-Control Effects With Tail On

With the addition of the tail to the model some of the force and moment coefficients due to the fully deflected (δ = 0.3 b/2) lateral controls were changed considerably. (See fig. 11.) The unfavorable yawing-moment coefficients due to the fully deflected controls changed to very favorable yawing-moment coefficients. Side-force coefficients

changed from positive to negative, and roll effectiveness was decreased about 20 to 28 percent at low angles of attack.

Inboard plain ailerons having chords of 30 percent of the wing chord and spans of 39.5 percent of the wing semispan have also been investigated on the model of the present tests. Unpublished results from these aileron studies indicate tail effects similar to those obtained in the present tests. These unpublished results also show that the addition of the vertical tail was primarily responsible for the changes in the yawing moments and side forces due to the lateral controls. However, both the vertical and horizontal tails contributed to the changes in the incremental rolling moments. These changes with the addition of the tail are apparently a result of the downwash effects from the deflected controls and an induced circulatory flow effect on the vertical tail.

Figure 11 also shows that, at the largest control deflection, the absolute magnitudes of ΔC_L , ΔC_D , and ΔC_m were reduced for most angles of attack when the tail was added to the model.

Speed-Brake Effects

Changing the speed-brake deflection from 0.2 b/2 to 0.3 b/2 approximately doubled the incremental drag coefficients at all Mach numbers throughout the angle-of-attack range. (See fig. 12.) Adding the tail had large effects on ΔC_m but rather small effects on ΔC_L and ΔC_D . The variation of both ΔC_L and ΔC_m with angle of attack appears to be large. These variations could probably be reduced by shifting the control hinge lines forward of the wing trailing edge and reducing the size of the upper controls.

CONCLUSIONS

An investigation has been made of several body-mounted lateral-control and speed-brake configurations on a 45° swept-wing model having a 4-percent-thick wing of aspect ratio 3. Six-component balance data were obtained at Mach numbers of 0.80, 0.94, and 0.98 for an angle-of-attack range that usually extended from about 0° to 21°. The results of the investigation indicate the following conclusions:

1. At large deflections, oppositely deflected body-mounted lateral controls produce fairly large rolling moments at low and moderate angles of attack even with speed brakes deflected 0.2 of the wing semispan.

- 2. Above the low angle-of-attack range, a lower body-mounted lateral control has higher roll effectiveness than an upper body-mounted lateral control when the controls extend along the wing trailing edge.
- 3. Shifting the oppositely deflected control hinge lines from 100 to 85 percent of the wing chord at the fuselage results in higher roll effectiveness at low deflections and decreased roll effectiveness for Mach numbers of 0.94 and 0.98 at large deflections.
- 4. The effect of reducing the span of the oppositely deflected controls 33 percent for a large control deflection was to decrease the roll effectiveness by about 20 percent at low angles of attack. At high angles of attack, the effectiveness of the shorter span controls approached or exceeded that obtained with the longer span controls.
- 5. Adding a complete tail to the model with oppositely deflected controls at large deflections caused a change in yawing moment from unfavorable to very favorable. The roll effectiveness, however, was decreased about 20 to 28 percent at low angles of attack.

Langley Aeronautical Laboratory,
National Advisory Committee for Aeronautics,
Langley Field, Va., August 16, 1956.

REFERENCES

- 1. Ward, Vernon G., Whitcomb, Charles F., and Pearson, Merwin D.: Air-Flow and Power Characteristics of the Langley 16-Foot Transonic Tunnel With Slotted Test Section. NACA RM L52E01, 1952.
- 2. Critzos, Chris C.: A Transonic Investigation of the Static Longitudinal-Stability Characteristics of a 45° Sweptback Wing-Fuselage Combination With and Without Horizontal Tail. NACA RM L56Al8, 1956.
- 3. Runckel, Jack F., and Lee, Edwin E., Jr.: Investigation at Transonic Speeds of the Loading Over a 45° Sweptback Wing Having an Aspect Ratio of 3, a Taper Ratio of 0.2, and NACA 65A004 Airfoil Sections. NACA RM L56F12, 1956.
- 4. Hallissy, Joseph M., and Bowman, Donald R.: Transonic Characteristics of a 45° Sweptback Wing-Fuselage Combination. Effect of Longitudinal Wing Position and Division of Wing and Fuselage Forces and Moments. NACA RM L52KO4, 1953.
- 5. Whitcomb, Charles F., and Osborne, Robert S.: An Experimental Investigation of Boundary Interference on Force and Moment Characteristics of Lifting Models in the Langley 16- and 8-Foot Transonic Tunnels. NACA RM L52L29, 1953.
- 6. Hallissy, Joseph M., Jr., West, F. E., Jr., and Liner, George: Effects of Spoiler Ailerons on the Aerodynamic Load Distribution Over a 45° Sweptback Wing at Mach Numbers From 0.60 to 1.03. NACA RM L54C17a, 1954.
- 7. Lowry, John G.: Data on Spoiler-Type Ailerons. NACA RM L53I24a, 1953.

TABLE I

LATERAL-CONTROL AND SPEED-BRAKE CONFIGURATIONS

	· · · · · · · · · · · · · · · · · · ·	
Model configuration	δ	Figure
Upper right and lower left controls; hinge line at 1.00cb, tail off	0.1 b/2, 0.2 b/2, 0.3 b/2	6
Upper right control; hinge line at 1.00cb, tail off	0.3 b/2	7
Lower right control; hinge line at 1.00c _b , tail off	0.3 b/2	7
Upper left and lower right controls; hinge line at 0.85cb, tail off	0.1 ъ/2, 0.2 ъ/2, 0.3 ъ/2	8
Upper right and lower left controls with control span reduced 1/3; hinge line at 1.00cb, tail off	0.2 b / 2	9
Upper right and lower left controls deflected 0.3 b/2 and upper left and lower right controls deflected 0.2 b/2; at 1.00cb, tail off		10
Upper right and lower left controls; hinge line at 1.00c _b , tail on	0.1 ъ/2, 0.2 ъ/2, 0.3 ъ/2	11
Speed brakes; hinge line at $1.00c_{\rm b}$, tail off	0.2 b/2, 0.3 b/2 ·	12
Speed brakes; hinge line at 1.00c _b , tail on	0.2 b/2, 0.3 b/2	12

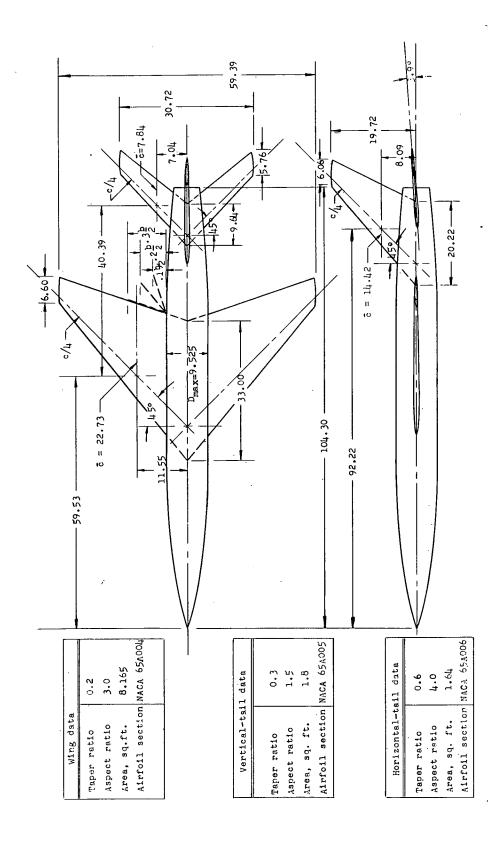
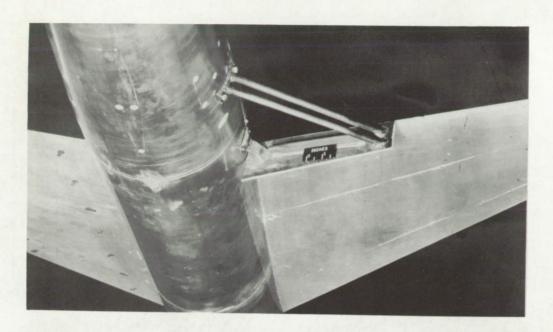
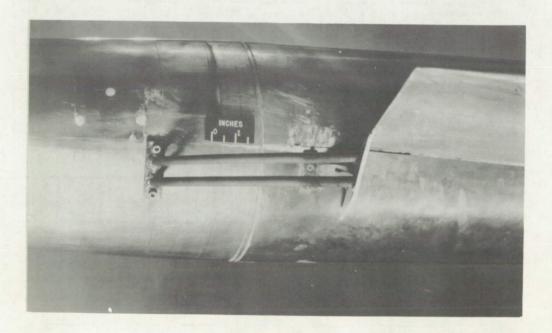


Figure 1. - Dimensional details of model. (All linear dimensions in inches.)



(a) Rear view.

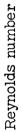
L-91472



(b) Side view.

L-91473

Figure 2.- Photograph showing a lower body-mounted lateral control. Hinge line at 1.00cb.



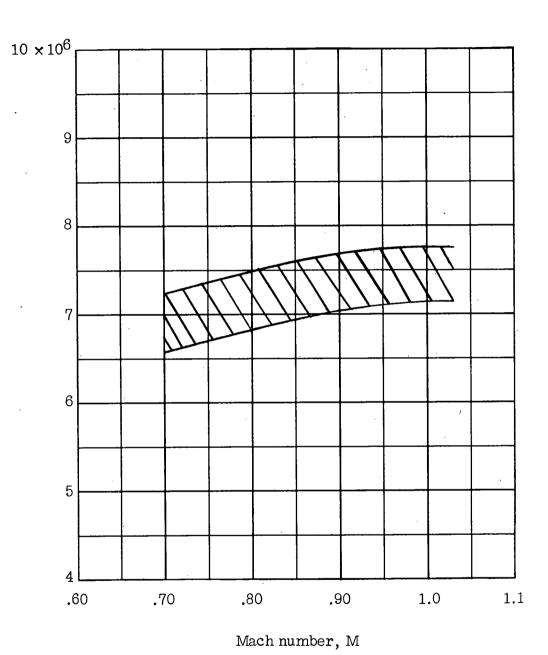


Figure 3.- Variation with Mach number of the Reynolds number (based on the mean aerodynamic chord) in the Langley 16-foot transonic tunnel.

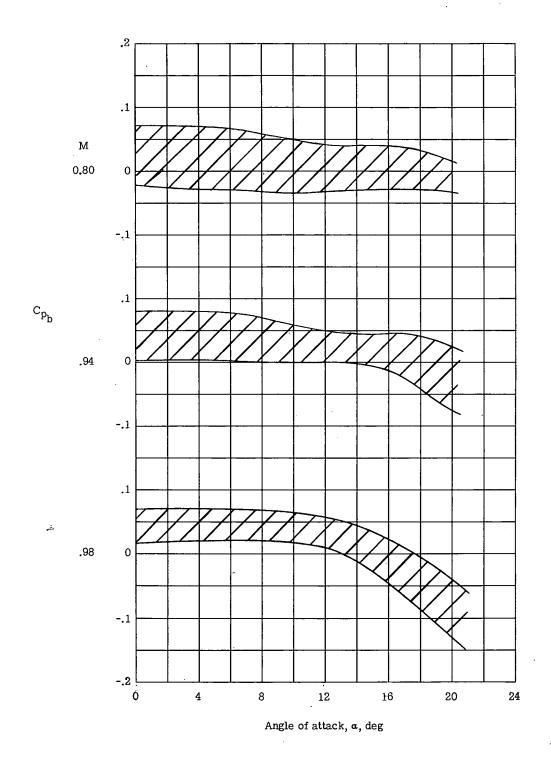


Figure 4.- Maximum variation with angle of attack of the average base pressure coefficients for all configurations for the three test Mach numbers.

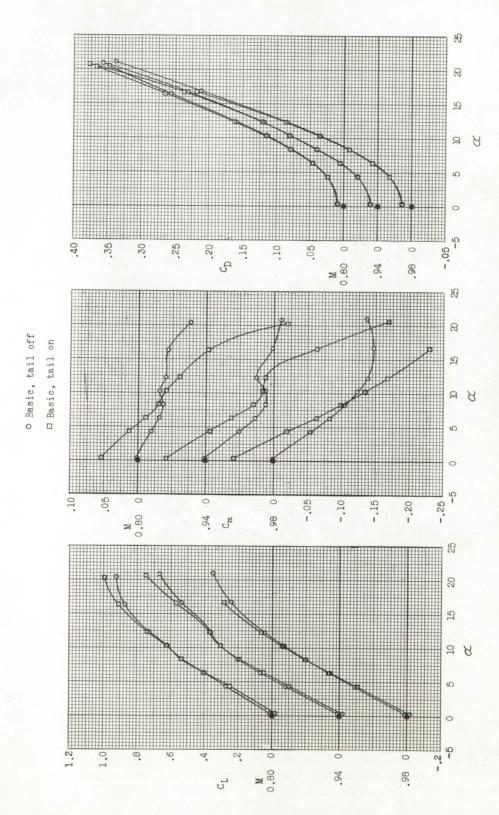
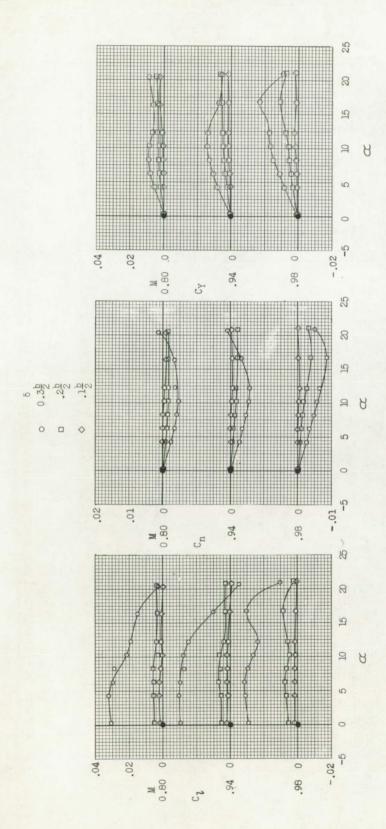
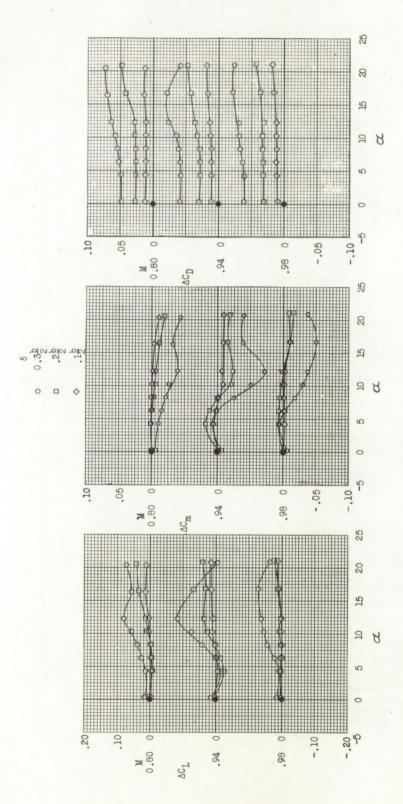


Figure 5.- Longitudinal aerodynamic characteristics for the basic tail-on and tail-off configurations.



(a) Lateral characteristics.

Figure 6.- Aerodynamic characteristics due to oppositely deflected controls at several deflections. Hinge lines at 1.00cb, tail off.



(b) Longitudinal characteristics.

Figure 6.- Concluded.

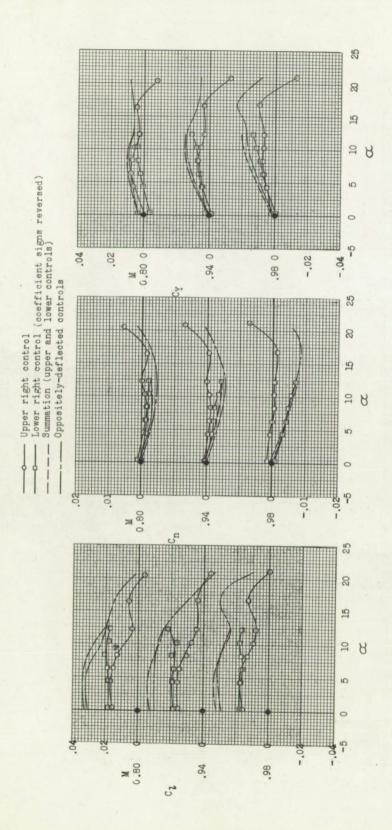
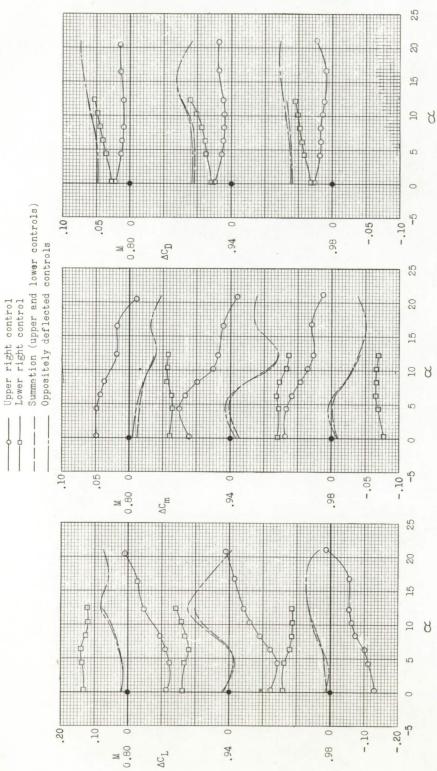


Figure 7.- Aerodynamic characteristics due to separately deflected con-Hinge lines at 1.00cb, tail trols at full deflection $(\delta = 0.3b/2)$. off.

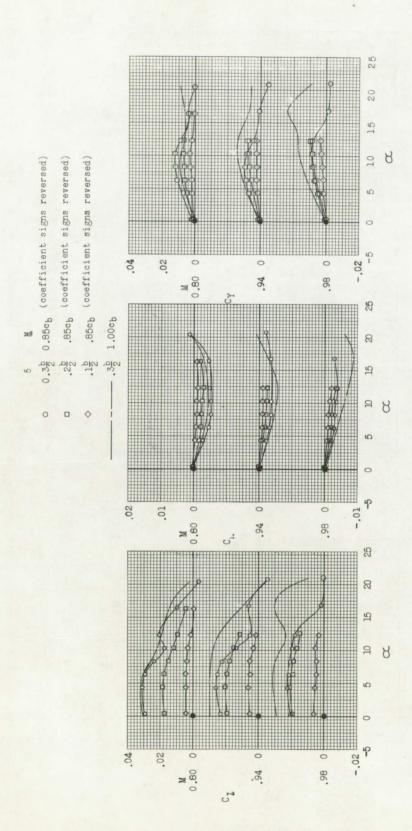
(a) Lateral characteristics.



(b) Longitudinal characteristics.

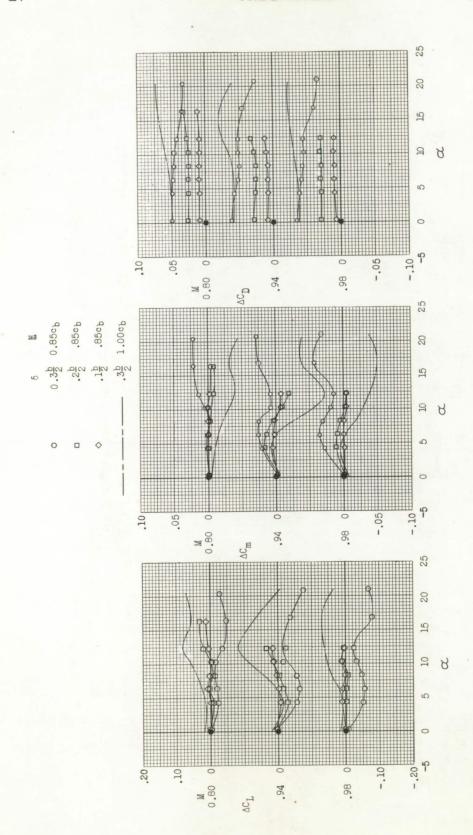
Figure 7.- Concluded.

CONFIDENTIAL



(a) Lateral characteristics.

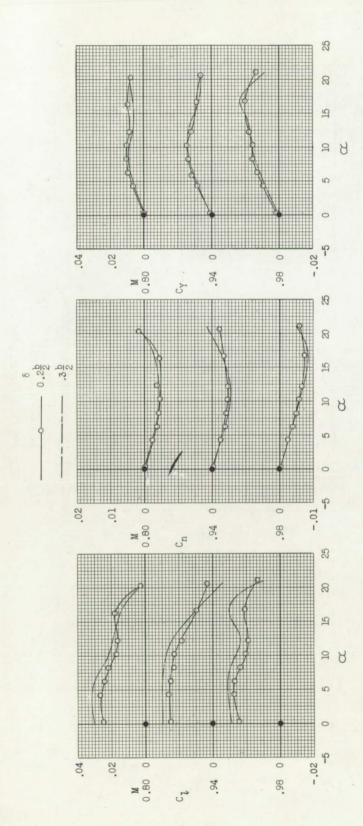
Figure 8.- Aerodynamic characteristics due to oppositely deflected controls at several deflections. Hinge lines at 0.85cb, tail off.



(b) Longitudinal characteristics.

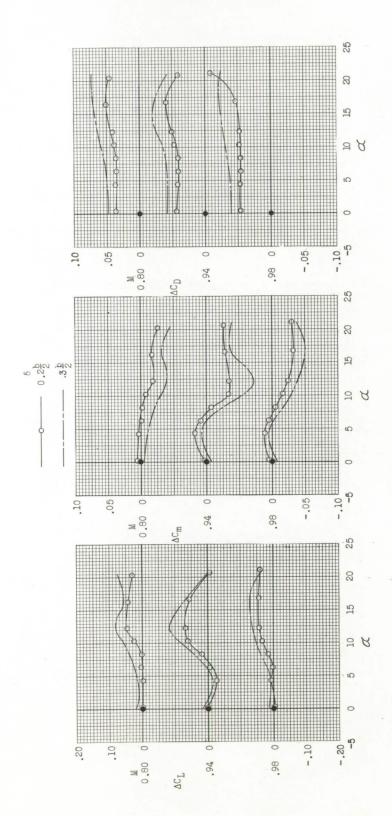
Figure 8.- Concluded.

CONFIDENTIAL



(a) Lateral characteristics.

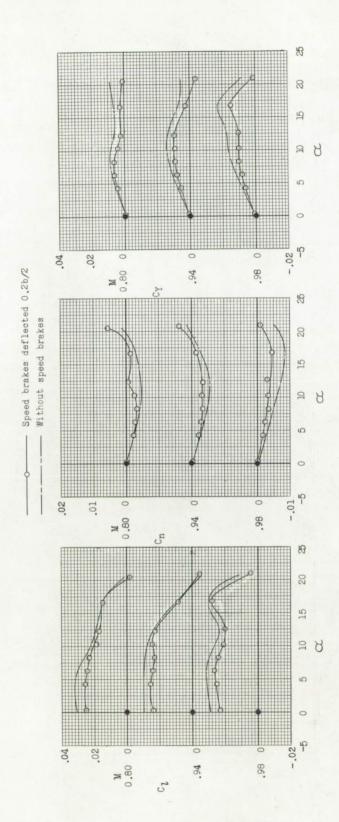
Figure 9.- Effect of reducing control span on aerodynamic characteristics Hinge lines due to oppositely deflected controls at full deflection. at 1.00cb, tail off.



(b) Longitudinal characteristics.

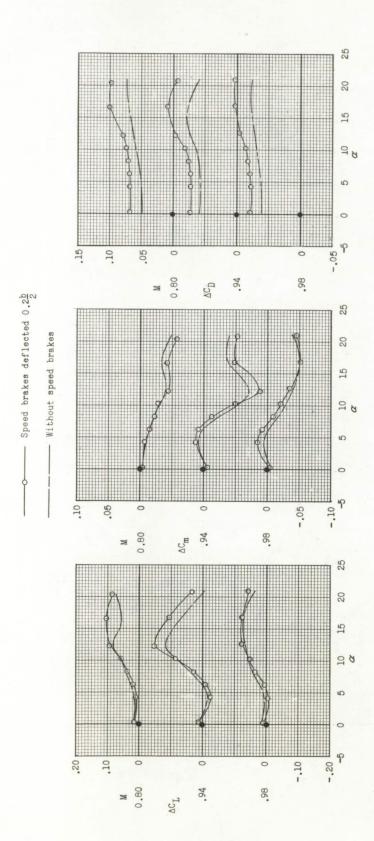
Figure 9.- Concluded.

CONFIDENTIAL



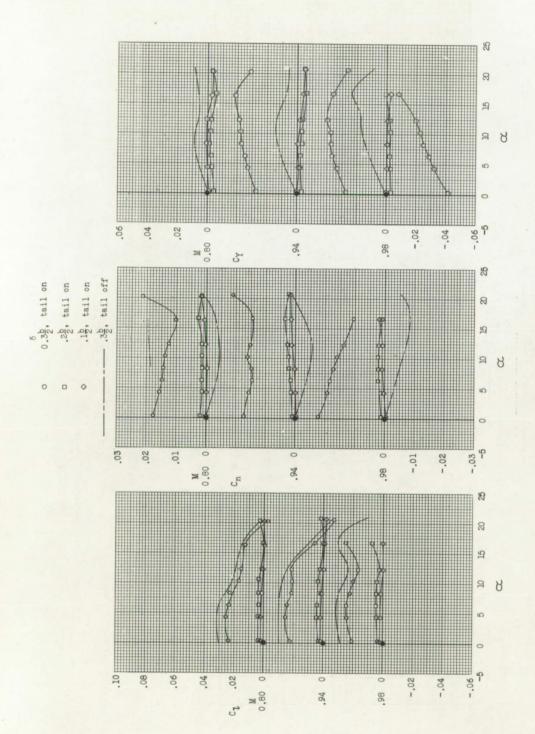
(a) Lateral characteristics.

Figure 10.- Effect of speed-brake deflection on aerodynamic characteristics due to oppositely deflected controls at full deflection ($\delta = 0.3b/2$). Hinge lines at 1.00cb, tail off.



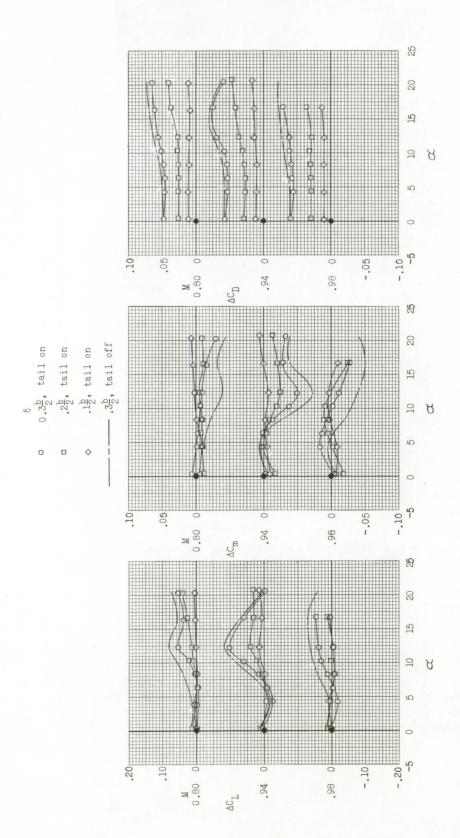
(b) Longitudinal characteristics.

Figure 10.- Concluded.



(a) Lateral characteristics.

Figure 11.- Aerodynamic characteristics due to oppositely deflected controls at several deflections. Hinge lines at 1.00cb, tail on.



(b) Longitudinal characteristics. Figure 11.- Concluded.

CONFIDENTIAL

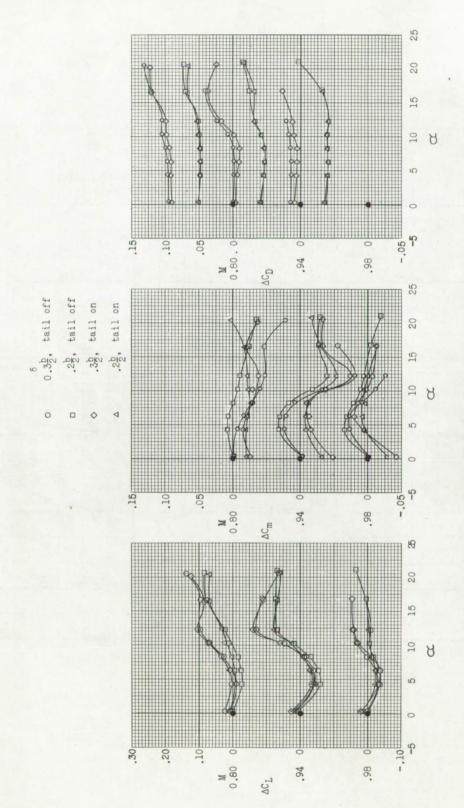


Figure 12. - Longitudinal aerodynamic characteristics due to speed brakes at two deflections with tail on and tail off. Hinge lines at 1.000cb.

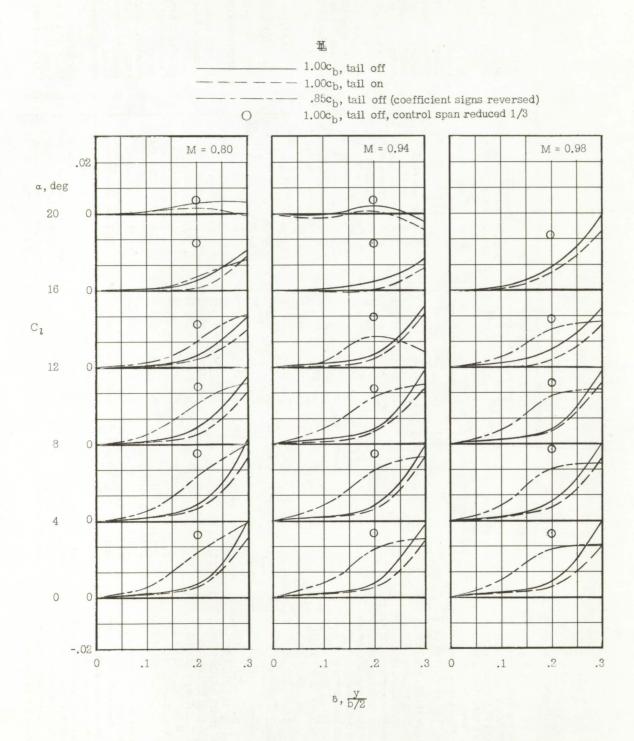


Figure 13.- Variation of rolling-moment coefficient with control deflection for several configurations.

CONFIDENTIAL